

ECONOMICAL ASSESSMENT of COMMERCIAL HIGH-SPEED TRANSPORT

Paula Margaretic

Airbus SAS

Data Scientist

1, Rond-Point Maurice Bellonte, 31707, BLAGNAC CEDEX, France, paumargaretic@gmail.com

Johan Steelant

ESA-ESTEC, Section of Aerothermodynamics and Propulsion Analysis, Keplerlaan 1, 2200AG Noordwijk, Netherlands, Email: johan.steelant@esa.int,

ABSTRACT

The potential future market demand for a high-speed aircraft along with an estimate of the related costs and ticket prices have been assessed. To address the future demand for a high-speed aircraft, the eligible origin and destination city-pairs and the potential network for such a vehicle have first been identified. Then, the number of premium passengers flying this network, over the next 20 years is forecasted. Based upon technical characteristics of the potential future high-speed aircraft, it is finally possible to determine the number of vehicles that would be necessary to accommodate this expected future demand.

1 INTRODUCTION

Since the dawn of aviation, mankind has been intrigued and motivated to cross long distances non-stop in a very short time. Driven by technology development in aerodynamics, propulsion and lightweight structures, commercial aircraft manufactures could gradually bridge longer ranges from coast-to-coast over trans-Atlantic up to trans-Pacific. However, the travel time did not necessarily follow the same trend as the cruise speed got stalled at around the sonic barrier. Concorde broke as first this paradigm for commercial aviation though this endeavour was lacking a commercial success. The fuel consumption is often too easily quoted as the basic reason, but one often forgets that the technologies deployed for Concorde were stemming from the late 50's and beginning of the 60's. Compared to subsonic aircraft designed in the 60's and 70's (such as Comet or DC-9), the Concorde was actually competitive in range despite its larger sfc. However, the political hurdles to get it deployed on routes with commercial interest at that time delayed its introduction dramatically and frightened the embracement of Concorde by other airliners. This unavoidably downsized the number of manufactured aircraft below the critical size needed to recover the development costs.

Meanwhile, ranges for subsonic aircraft designed in the 90's have almost doubled, mainly due to improved aerodynamical designs, availability of light-weight and high-temperature materials, lower sfc due to higher bypass ratios, higher TIT, etc. Similar improvements could be applied to a successor of the Concorde to improve its sfc or range for the same flight speed [1][2]: implementation of a bypass ratio instead of none, application of more advanced cooling concepts for turbine blades, use of light-weight heat resistant materials, use of a Variable Cycle Engine rather than using an afterburner or reheat...

Less known to the public is that these kind of prospective studies were carried out to improve the performance of the Concorde already four months after the start of scheduled services in 1976. This project should lead to the Concorde B model based upon modifications on aerodynamics, systems,

weight, fuel tanks and the propulsion unit This should allow the operating range, primarily designed for the connection Paris/London-New York, to be increased to allow connections of the type (see **Figure 1**):

1. Other European capital cities - East Coast of the US in one sector
2. United States - Japan in two sectors
3. Europe - Australia in three sectors



Figure 1: Increased range of Concorde B (right) compared to original Concorde (left) with implementation of contemporary technologies in 1976 [1].

The above is an example of how the economic viability of any aircraft system throughout its lifetime is largely dependent on the timely introduction of contemporary technologies.

Despite the mothballing of Concorde, there is worldwide a regained interest in commercial high-speed transportation ranging from supersonic business jets (ref. HISAC, US, Russia), up to hypersonic speeds. During the last 10 years, the European Commission has co-funded long-term research projects on commercial high-speed transportation such as ATLLAS I and II [4], LAPCAT I and II [5][6] and FAST20XX [7]. Also, national activities such as the ZEHST program in France [8] or the JAXA Hypersonic Transport (HST) in Japan [11] indicate the need and wish to establish the required basic technologies, as well as the design of conceptual vehicles to improve their overall performance. As the above projects have grown towards a certain maturity in conceptual layout and basic proof of technical feasibility, their performance figures in terms of ranges, speed, capacity, etc allow to preliminary assess their economic viability in an operational environment.

In this context, European and Japanese researchers have teamed up to map a path for developing high-speed air travel in a joint EC-Japan funded project HIKARI. One of the HIKARI work groups deals with the estimation of the demand and operating costs, based on high-level requirements, in order to provide insights as to the economic viability of high-speed transport. This will feed a second activity, which will provide elements to justify the economic interest of high-speed transport and gain public acceptance. They will also look at potential technologies, environmental impact, and other factors to provide a vision of our transport of the future.

Relying on the results already obtained by the HIKARI consortium, the aim of this paper is to assess the potential future market demand for a high-speed aircraft and estimate the costs and ticket prices of such a vehicle. To address the potential future demand for a high-speed aircraft, the eligible origin and destination city-pairs (OD CPs) and the potential network (hereafter, HIKARI network) for such a vehicle need to be identified first. Then, the number of premium passengers flying over this network, during the next 20 years is forecasted. Based upon technical characteristics of the potential future high-speed

aircraft, it is finally possible to determine the number of vehicles that would be necessary to accommodate this expected future demand.

To estimate the cost and ticket price, one of the HIKARI partners Oxford Economics, follows the methodology adopted by REL in a 2008 study, using the LAPCAT concept, updating financial and economic variables for latest data, and amending certain technical assumptions (on utilization rates, load factor and seating capacity).

At first, the market study methodology is worked out enabling the assessment of the potential future market for a high-speed aircraft, together with the estimation of cost and ticket price. This is followed by a market study. More specifically, the HIKARI network is evaluated enabling the forecast of the number of high-speed aircraft, assuming an exogenous market share capture. Once cost and ticket price are established, the market share capture model can be detailed. With these elements available, the market share capture model together with the ticket price estimation model allows determining the equilibrium of the market, defined as a vector of ticket price, market share and expected number of vehicles necessary to accommodate this identified market. Conclusions and way forward are in the last section. Supportive and complementary information is relegated to the appendix.

2 MARKET STUDY METHODOLOGY

A dedicated market study is needed to compute the expected number of vehicles necessary to accommodate the forecasted demand for a potential future high-speed aircraft over the next 20 years. The market study is worked out along 5 major lines:

1. Identification of the HIKARI network, the eligible origin-destination (OD), city-pairs (CPs) and the expected number of first class and business (FC+B) passengers that are expected to fly the identified CPs in the coming 20 years' time.
2. Determination of the expected future number of vehicles that would be necessary to accommodate the forecasted FC+B passengers assuming an exogenous market share capture per cent.
3. Estimation of the development and operating costs based on the methodology developed by REL (2008), together with ticket price at which such a future vehicle could operate,
4. Building of a discrete choice model to estimate the market share that a high speed aircraft could capture from existing commercial aircraft.
5. Theoretical determination of the market equilibrium: i.e. combination of the market share capture model with the ticket price estimation model in order to determine,
 - a. the market share that the high speed vehicle could capture from the HIKARI network;
 - b. re-compute the expected number of vehicles necessary to accommodate this identified market
 - c. the ticket price at which such a vehicle could operate.

In the following paragraphs, we detail each of the above steps.

2.1 Potential HIKARI Network and OD CPs

To identify the potential HIKARI network and the eligible OD CPs in this network, we follow three steps. First, we forecast the expected future number of premium passengers, per OD CP (the market size). Second, we construct valid itineraries (routes)¹ for each OD CP. Finally, by predicting the percentage of

¹ An itinerary is a flight or a sequence of connecting flights used to travel between any two cities.

travellers that are likely to select each itinerary, at each city-pair; we determine the demand of each itinerary, which in turn determines the shape of the potential future HIKARI network.

1.1.1 Market size

We focus on international long haul², premium air passengers, as of 2012. The data source for 2012 premium air passenger flows is Sabre Airline Solutions® proprietary data intelligence solution, Global Demand Data (GDD),³ which provides air travel itineraries between airports all over the world, since 2002. Then, relying on Airbus GMF 20-year air traffic forecast at CP level⁴, we forecast the expected number of premium passengers, per OD CP, in 2032. In particular, we restrain to international long-haul OD city-pairs, with at least 3200 monthly, bi-directional premium passengers in 2032.

1.1.2 Itinerary construction

Once the size (number of passengers) of each market (OD CP) has been forecasted, the next step is to construct valid itineraries (routes) for each OD CP. Following Mathiasel [15], Schmitz et al. [16] and Grosche [14], we develop a set of rules for itinerary building, as follows.

Number of stops:

In general, passengers want to minimize their travel time and to increase the convenience of the journey. Thus, if there are too many stops within a sequence of flights, this sequence (itinerary) is unlikely to be chosen by the passenger. The maximum number of stops s_{max} thus excludes connection flights with more intermediate stops than this number. Because several stops with only one HIKARI leg would outweigh the time gain of a high-speed aircraft, we choose $s_{max} = 1$.

Detour:

In general, each sequence of connecting flights represents a detour compared to the direct flight between two cities. A maximum detour factor d_{max} indicates to what extent the geographical total distance of the sequence of connecting flights $dist_{cnx}$ might exceed the direct distance $dist_{dir}$ between the origin and destination cities: $dist_{cnx} \leq d_{max} \times dist_{dir}$. The detour factor leads to a pre-selection of possible HIKARI itineraries. We assume $d_{max} = 1.4$ i.e. the great circle (GC) distance of the connecting leg and the HIKARI leg can be at most 40% larger than the direct OD GC distance.⁵

Recall that $s_{max} = 1$.

Connection time:

For simplicity and because we assume a full and optimized connectivity between connecting leg and HIKARI leg, the connection time t_{cnx} is set at 2 hours.

The following table summarizes the selected values of the parameters.

Coefficient	Value
s_{max}	1.0
d_{max}	1.4
t_{cnx}	2.0

² By international long haul city-pairs, we mean all CPs with GC distance above 3700km

³ GDD aggregates information from world distribution systems, like Sabre, Amadeus and Galileo and performs adjustments to estimate total demand.

⁴ Airbus' GMF traffic forecast gives the overall shape of the expected traffic evolution over the next 20 years.

⁵ The value of the detour factor is in line with the calibrated detour factor in Grosche (2009).

Table 1: Parameters of the itinerary construction (Source: Airbus)

1.1.3 HIKARI network forecast

Once itineraries for each OD CP have been built, the share that each itinerary has on the market (OD CP) is determined based on the elapsed flight time. Intuitively, the longer the flight time of a given itinerary, the less likely it is that a passenger would select such an itinerary.

The demand of each itinerary is determined by multiplying the percentage of passengers expected to travel on each itinerary by the expected market size i.e. the number of OD, city- pair air passengers. The aggregation of itineraries and OD CP determines the shape of the expected future HIKARI network.

2.2 Expected Future Number of Aircraft based upon an Exogenous Market Share Capture

Relying on the HIKARI network the expected future number of high-speed vehicles needs to be determined necessary to accommodate the forecasted FC+B passengers, assuming an exogenous market share capture per cent. Importantly, we first focus on traffic within the HIKARI legs to get a feel about the potential market without being subject to any constraint on ticket price or other external variables affecting the market share. Several additional assumptions were taken at this stage⁶:

1. Two vehicle capacities, 100 and 300 seats.
2. Two speed clusters for the high speed aircraft:
 - a. Cluster 1 has an average speed of 4260 km/h, i.e. covering Mach 3 to 5 aircraft
 - b. Cluster 2 has an average speed of 7100km/h, i.e. covering March 6 to 8 aircraft
3. Two aircraft utilization values, i.e. 3150 and 5000 block hours per year
4. 3 and 5 weekly flight frequencies, per HIKARI leg
5. Additional dwell time on ground per high-speed aircraft and per day is of 6h

The flight time computation formula used for each cluster follows:

$$\begin{aligned} \text{Flight time Cluster 1} &= \frac{1}{4260} \times (\text{GC distance} - 966\text{km}) + \frac{51}{60} \\ \text{Flight time Cluster 2} &= \frac{1}{7100} \times (\text{GC distance} - 966\text{km}) + \frac{51}{60} \end{aligned}$$

Finally, regarding eligible airports to be considered as hubs in the HIKARI network, they must satisfy the following conditions:

- Airport's distance to the coast is smaller than 400 km,^{7,8}
- Each airport in the HIKARI network has at least 3 HIKARI legs.

⁶ These assumptions are in line with the HST aircraft conceptually designed by the partners of the HIKARI consortium and the resulting classification of HST aircraft capabilities and operational exploitation.

⁷ The constraint distance to the coast is due to sonic boom or ground overpressure produced by hypersonic flight. See LAPCAT (2008) for a discussion.

⁸ As robustness check, we also consider 300 km.

2.3 Cost and Ticket Price Estimation

The ticket cost model estimation is based on the LAPCAT concept, with development and production costs estimated by REL, taken from a 2008 report by ESA-ESTEC.⁹ This study found an initial development cost of €22.6bn and a first unit price of €979m (2006 prices).

These figures have been uprated, in line with the cost of investment goods in the French aerospace sector to 2012 prices. Combined with an assumed 90% learning factor¹⁰, applied financial assumptions, including a 15 year asset life and 5% interest rate, these yield a relationship between the production run and the aircraft purchase cost.

Variable costs have subsequently been added. The key cost here is fuel, assumed to be 170,000kg of hydrogen per one way trip from Europe to Australia for a 300seat vehicle, costing €4.49 per kg to produce in 2012 prices. This assumption is based on the theoretical efficiency of hydrogen produced via electrolysis, rather than current small-scale production – an assumption made by REL and reported in detail by ESA-ESTEC. No differentiation on hydrogen consumption based on the different classes of vehicles has been introduced.

Maintenance costs are assumed to be 0.005% of the purchase price of the plane per one-way trip, with an additional once a year service costs of 10% of the purchase price. Finally, there are indirect costs associated with running an airline such as slot fees, head office functions, and so on. These are estimated at €30.7m per annum, uprated from REL's 2006 estimate, in line with the French aviation sector Gross value added (GVA) deflator.

These costs are then combined with assumptions over the working time of the aircraft and passenger load. Two single flights per aircraft and per day are assumed, with 30 days per year down time, yielding 550 flights per annum. Also, a load factor of 75% is supposed. Finally, each ticket is marked up by 5% on cost price to yield ticket price.

These assumptions jointly deliver the relationship between aircraft produced and ticket price, to be discussed in more detail in section 2.3.

2.4 Market Share Capture Model

To estimate the market share that a high-speed aircraft could capture from the expected future premium air passenger market, we solve the theoretical problem of an individual, who wants to travel by air and has to decide between a subsonic and a high-speed aircraft. More specifically, we suppose that his random utility depends linearly on the flight time and the airfares he pays for the trip.¹¹ Assuming that the error in his random utility function is distributed logistic, it is possible to show that the probability that he prefers the high-speed aircraft takes the following form:

$$Prob(HST_i) = \frac{1}{1 + e^{\beta_0 + \beta_1 * time\ ratio + \beta_2 * fare\ ratio}}$$

⁹ See <http://cordis.europa.eu/documents/documentlibrary/120142511EN6.pdf>

¹⁰ Intuitively, the learning factor means that a doubling of the production run reduces cost by 10%.

¹¹ For details on discrete choice models, see Train (2009).

where $Prob(HST_i)$ is the probability that an individual i chooses the high-speed transport, *time ratio* is the proportion between travel time of high speed and subsonic aircraft, while *fare ratio* corresponds to the ratio between airfare in a high speed and a subsonic aircraft.

In order to calibrate the value of the coefficients β_0 , β_1 and β_2 , we use Concorde data between 1984 and 2002. More specifically, due to data availability, the Concorde routes used for the calibration were London-Washington and New York-Paris.

2.5 Theoretical Equilibrium Determination

By combining the above presented models, the equilibrium in the market can be calculated which is defined as a vector:

$$E^* = (Ticket\ price^*, Market\ share^*, Number\ of\ aircraft^*).$$

More specifically, to determine the equilibrium, the following system of 3 equations, with 3 unknowns (*Ticket price**, *Market share**, *Number of aircraft**) is to be solved:

- (1) $Ticket\ price = f(Number\ of\ aircraft, a)$
- (2) $Market\ share = g(Ticket\ price, b)$
- (3) $Number\ of\ aircraft^* = h(Market\ share, c);$

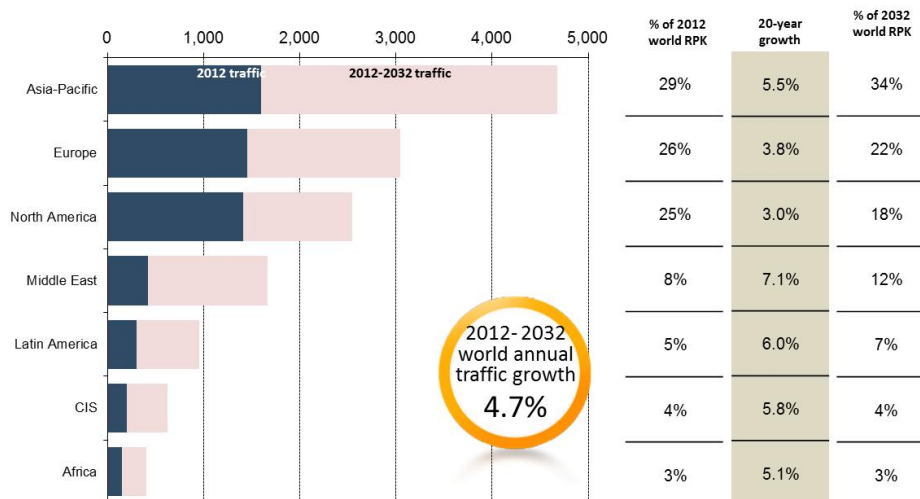
with a , b and c fixed parameters, including load factor, aircraft capacity, speed (time ratio), etc.

3 MARKET STUDY METHODOLOGY

Each of the steps within the followed market study methodology is addressed consecutively and discussed in detail below.

3.1 Potential HIKARI Network and OD CPs

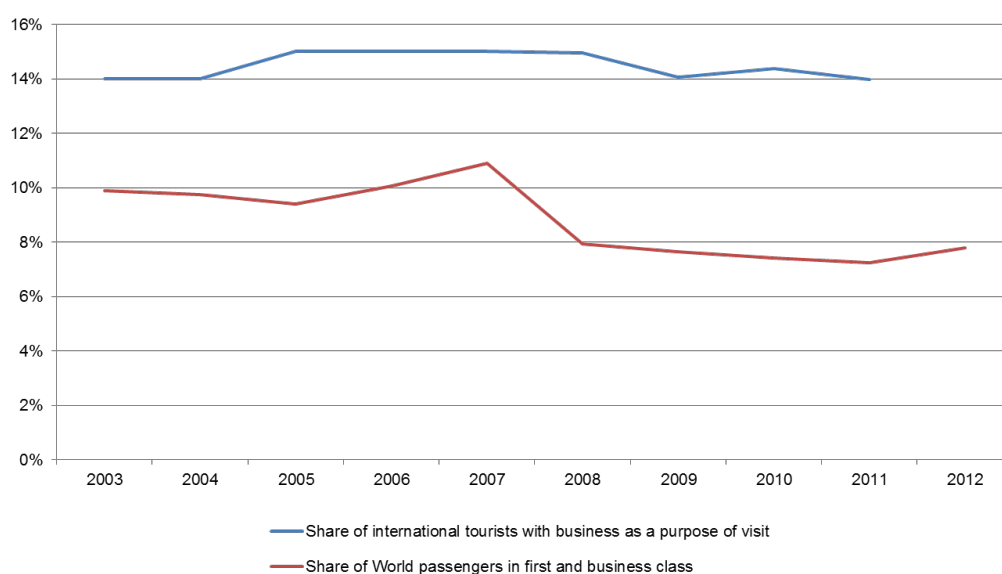
Figure 2 depicts overall GMF 2013 traffic forecast results, which are used to forecast the expected number of FC+B passengers in 2032. It shows that over the next 20 years, air traffic is expected to grow at a 4.7% annual pace. According to Airbus GMF, Asia-Pacific will lead air traffic growth, representing 34% of world RPK in 2032. Together with Europe and North America, these three regions will represent ~75% of 2032 world RPK.



Source: Airbus GMF 2013.

Figure 2: RPK traffic by airline domicile (billions).

Because the potential future demand for a high-speed aircraft targets premium passengers, **Figure 3** depicts the evolution of the share of these passengers on total air passengers, over the last 10 years. Importantly, we assume that the ~8% share of premium passengers will remain constant over the next 20 – 35 years. Reinforcing the previous assumption, figure 2 also shows that the proportion of international tourists, with business as purpose of visit, has remained stable over the same period.



Source: UNWTO, GDD Sabre, Airbus.

Figure 3: Evolution of FC+B passengers and tourists with business purpose (in %).

To characterize the HIKARI network and the eligible OD CPs, we focus on four dimensions:

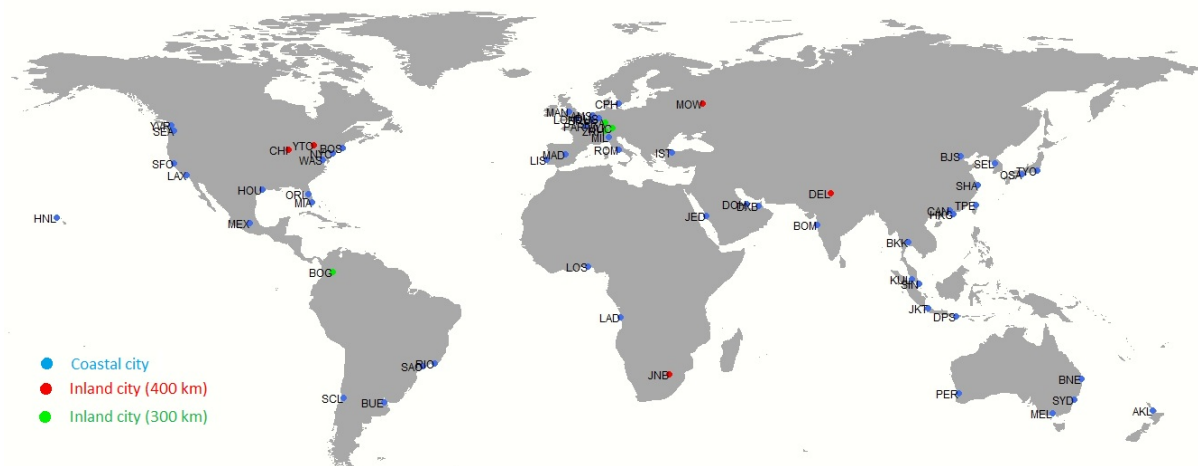
- Identification of HIKARI hubs
- Expected traffic growth over the eligible OD CPs
- The resulting HIKARI network
- Distribution of premium passengers in the HIKARI network, by distance

3.1.1 Identification of HIKARI hubs

Figure 4 depicts the 56 HIKARI hub cities identified, all of which satisfy the constraints stated in sections 1.2 and 1.3. These HIKARI hubs are used to build valid itineraries for each OD CP. The names of the cities, abbreviations and distance to the coast for each city are displayed in the appendix, together with a zoom in Europe (see annex). Interestingly, the constraint distance to the coast (300km or 400km) does not significantly alter the number of eligible HIKARI cities. More specifically, assuming a 300km distance constraint, the number of HIKARI hubs reduces to 52, 4 cities less than if supposing 400km.

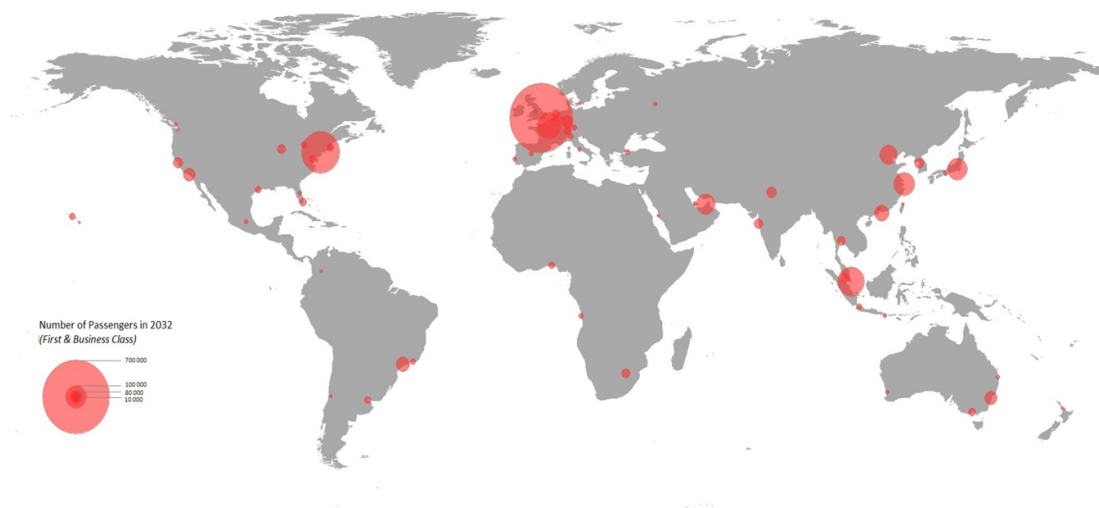
Figure 5 displays the expected future size of the HIKARI cities, as measured by forecasted monthly premium passengers departing from each of the HIKARI cities, in 2032.

It is worth highlighting that all the HIKARI cities are already aviation mega cities, according to the GMF definition, i.e. cities that handle more than 10,000 long-haul passengers per day (both premium and economy passengers).



Note: Airport/city codes, with distance to the coast lower than 400 km.

Figure 4: Eligible HIKARI cities satisfying the constraint distance to the coast lower than 300 and 400 km.

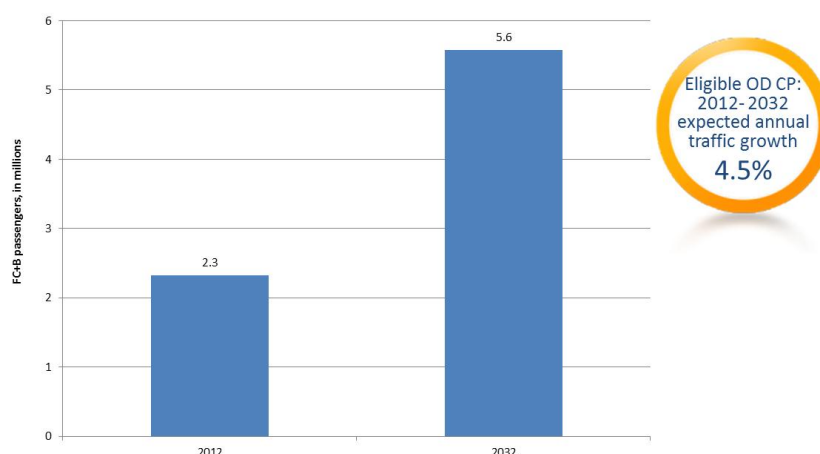


Source: Airbus GMF 2013.

Figure 5: HIKARI cities and expected monthly premium passengers, in 2032.

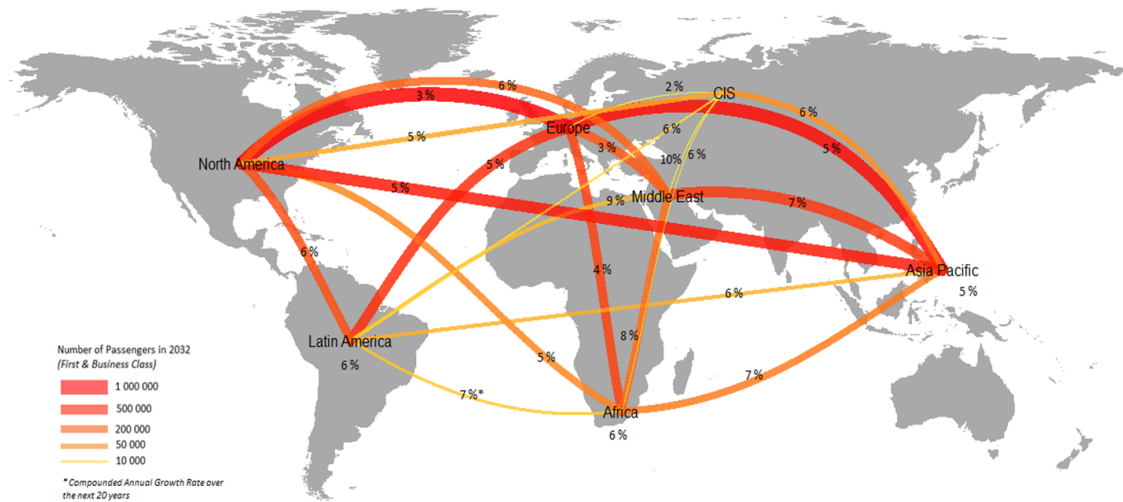
3.1.2 Expected traffic growth over the HIKARI network

Figure 7 shows 2012 and 2032 estimated premium passengers, over the eligible OD CPs, as stated in section 1.1. These premium passengers are forecasted to expand 4.5% annually, over the next 20 years. **Figure 8** details further **Figure 7**, by distinguishing between region pairs. It also displays the compounded annual growth rate, per region pair, over the period.



Monthly premium passengers, as of September 2012. Source: Airbus GMF 2013.

Figure 6: Monthly premium passengers over the identified OD CPs, 2012, 2032 and 2048, in millions.



Source: Airbus GMF 2013.

Figure 7: Monthly premium passengers over the identified OD CPs, by region pairs, in millions.

3.1.3 The resulting HIKARI network

Figure 8 and **Figure 9** display the expected future HIKARI network, which comprises 151 countries, 1095 country-pairs, 506 cities, 4768 OD city-pairs and 18810 routings.

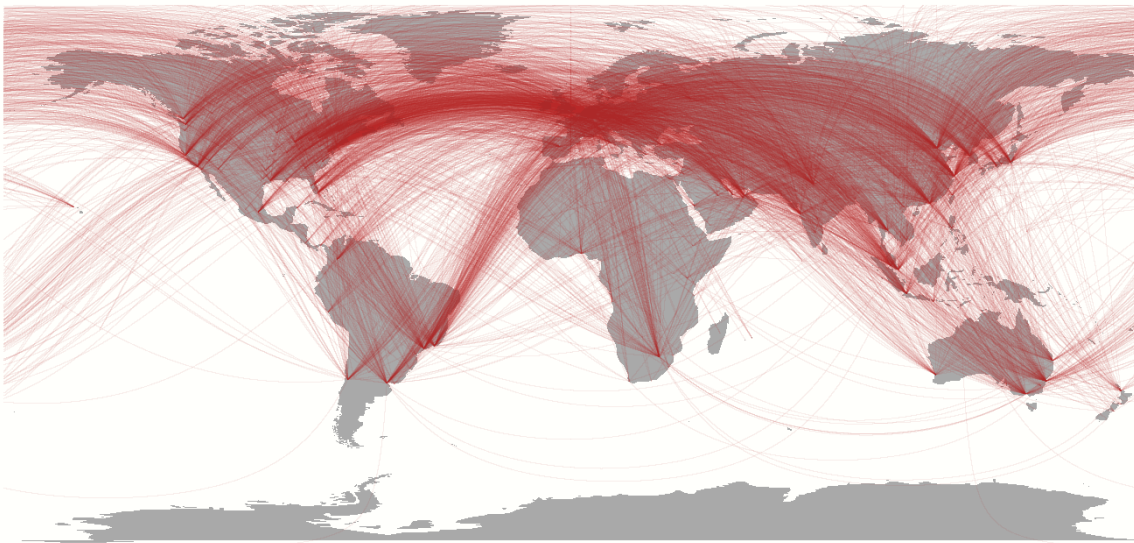


Figure 8: HIKARI network in 2032, with ~ 4800 eligible OD, city pairs. Source: Airbus GMF 2013.

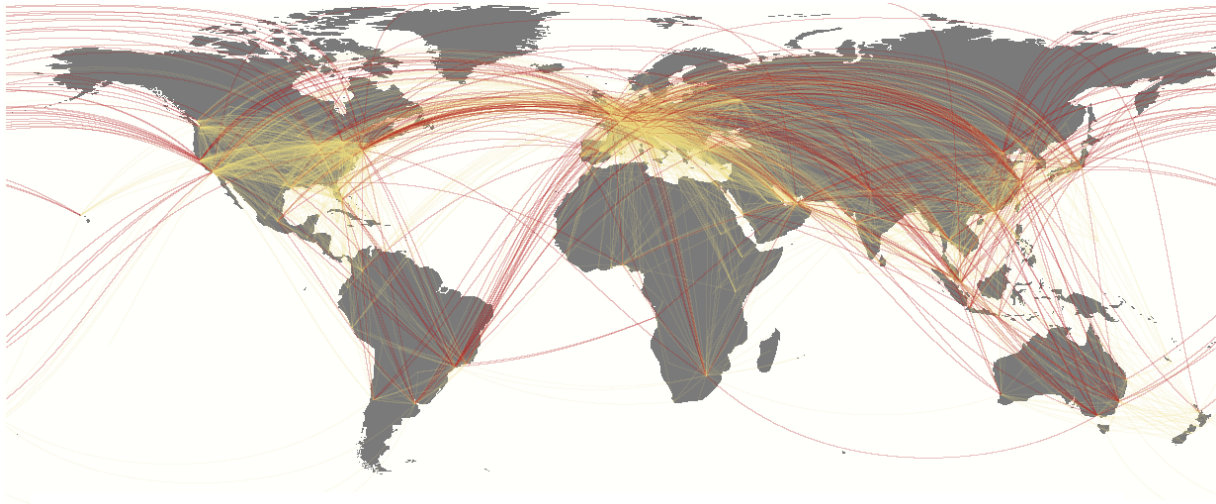
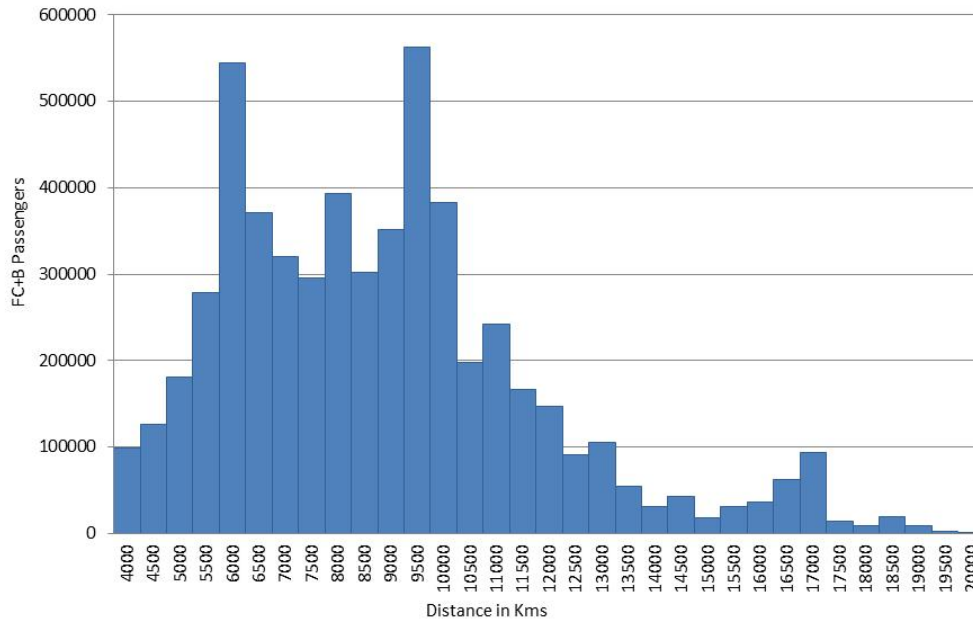


Figure 9: HIKARI network. Hypersonic legs (in red) and feeding legs (in yellow), 2032 (Source: Airbus GMF 2013).

3.1.4 Distribution of premium passengers in the HIKARI network, by distance

It is also worth looking at the distribution of the forecasted premium passengers by distance as plotted in **Figure 10** on the basis of the Great Circle distance. For the real distance flown, the great circle distance should roughly be multiplied with a distance factor of 1.4 to indicate the range that the aircraft would technically be capable to cover.



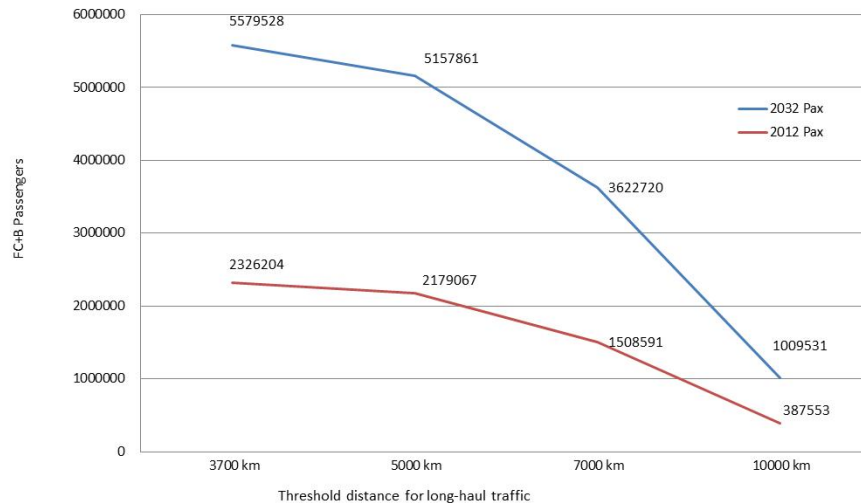
Source: Airbus GMF 2013.

Figure 10: Premium passenger distribution in 2032 by shortest distance (in km) i.e. along great circle distance.

As shown in **Figure 10**, the distribution of premium passengers is skewed to the right (skewness coefficient of 0.92), with two peaks corresponding to the intervals 6,000-6,500 and 9,500-10,000 kilometres for GC distance, i.e. 8,500km and 14,000km real flight trajectory. The fact that there is also a distinct long right tail of the premium passenger distribution underlines the potential for high-speed aircraft, as its flight time gain relative to the subsonic aircraft increases with distance.

It is now possible to relate **Figure 6**, **Figure 7** and **Figure 10** to investigate the sensitivity of the predicted premium passengers to different assumptions on the threshold distance to consider for international long-haul traffic.¹² **Figure 11** displays the reduction in the expected premium passengers if, instead of considering a GC-distance of 3700 km, it is assumed 5000, 7000 or 10000 km (GC-distance).

¹² Recall that international long-haul traffic includes all city-pairs with GC distance above 3700km.



Source: Airbus GMF 2013.

Figure 11: Sensitivity of premium passengers to threshold distance (Great Circle Distance)

3.2 Expected Number of Aircraft, Assuming an Exogenous Market Share Capture

The expected number of high-speed aircraft necessary to accommodate the forecasted demand is determined assuming an exogenous market share capture¹³. This is done both for cluster 1, which aircraft has an average speed of 4260 km/h, and cluster 2, with an average speed of 7100 km/h.

3.2.1 Results for Cluster 1

Figure 12 displays the forecasted number of aircraft, as a function of the (exogenous) market share that this aircraft could attain. Both figures assume an aircraft capacity of 100 seats. For completeness, the figures display market share per cents in the interval [0,100]. The difference between both figures is the assumption on yearly utilization hours: 3150 hours per year (left) versus 5000 hours (right). Combined, they show that a higher utilization of the high-speed aircraft results in less forecasted vehicles to accommodate the same premium passenger demand.

¹³ Section 2.4 presents the market share capture model, which substitutes the exogenous market share assumed here.

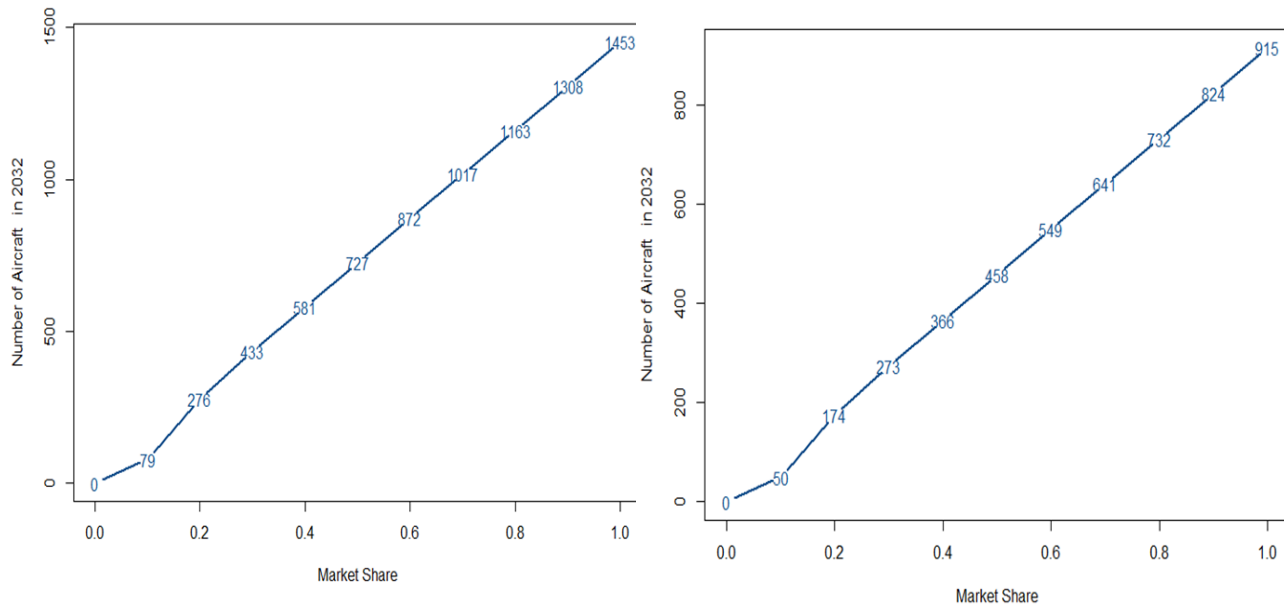


Figure 12: Forecasted number of cluster 1 aircraft in 2032, assuming 3 weekly frequencies; an aircraft capacity of 100 seats, load factor of 75%; yearly utilization hours: 3150h (left) and 5000h (right).

Figure 13 also displays the forecasted demand for a high-speed aircraft, as a function of market share, but instead assuming an aircraft capacity of 300 seats. It compares the situation with 3150 yearly utilization hours and 5000 yearly utilization hours.

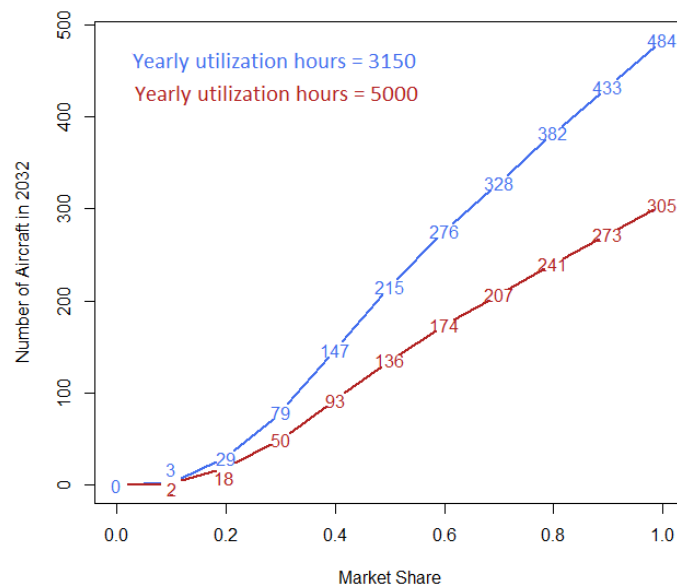


Figure 13: Forecasted number of cluster 1 aircraft in 2032, assuming 3 weekly frequencies; an aircraft capacity of 300 seats, load factor of 75%; yearly utilization hours: 3150h (left) and 5000h (right).

Importantly, the few predicted vehicles under the assumption of 300 seats are due to the way we compute expected future vehicles. More specifically, we assume that if annual forecasted premium passengers on a given route are not enough to fill the annual theoretical seats that would be offered by such a vehicle on the same route, the route is discarded.

Overall, **Figure 12** to **Figure 13** show that there exists a market for a potential future high-speed aircraft. However, the size of this market, as measured by the number of forecasted high-speed aircraft in 2032, strongly depends on the assumptions taken. As an illustration, assuming an aircraft capacity of 100 seats and a potential market share between 10% and 20%, the number of expected aircraft ranges between 50 and 276 vehicles.

The significant variability of the results is the reason why the next subsection investigates how results change when the aircraft speed change, relative to the baseline scenario. The baseline scenario is characterized by the following parameters: an average speed of 4200 km/h, an aircraft capacity of 100 seats, 3 weekly frequencies, 3150 yearly utilization hours and a load factor of 75%.

3.2.2 Results for Cluster 2

Figure 14 and **Figure 15** compare the results of cluster 1 and cluster 2, in terms of forecasted number of aircraft. They assume a 3 and a 5 weekly frequencies and a load factor of 75%. **Figure 14** supposes an aircraft capacity of 100 seats, whereas **Figure 15** assumes an aircraft capacity of 300 seats.

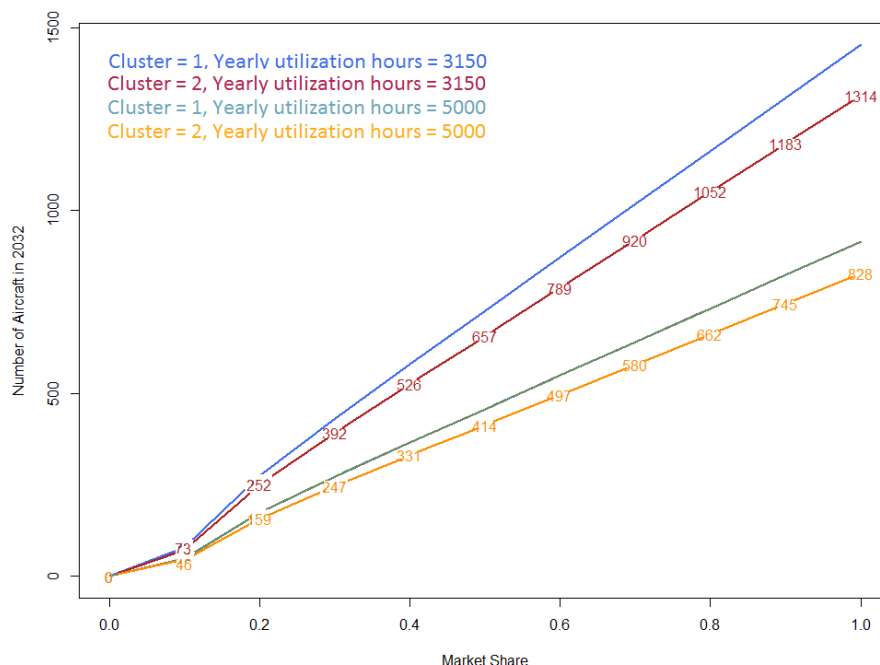


Figure 14: Comparison between results of cluster 1 and cluster 2, in terms of forecasted number of aircraft in 2032. Assumptions: 3 weekly frequencies; aircraft capacity of 100 seats; load factor of 75%; Cluster 1, with an average speed of 4260 km/h; Cluster 2, with an average speed of 7100 km/h.

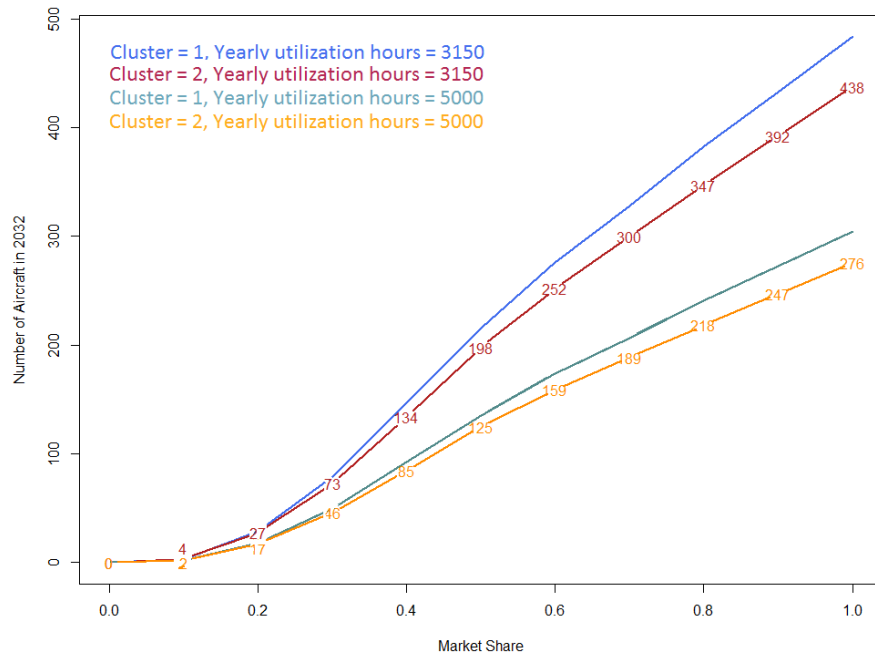


Figure 15: Comparison between results of cluster 1 and cluster 2, in terms of forecasted number of aircraft in 2032. Assumptions: 3 weekly frequencies; aircraft capacity of 300 seats; load factor of 75%; Cluster 1, with an average speed of 4260 km/h; Cluster 2, with an average speed of 7100 km/h.

A higher vehicle velocity, relative to cluster 1, leads to less forecasted aircraft. Intuitively, flying faster results in less yearly utilization hours and therefore, result in a lower number of needed high-speed vehicles.

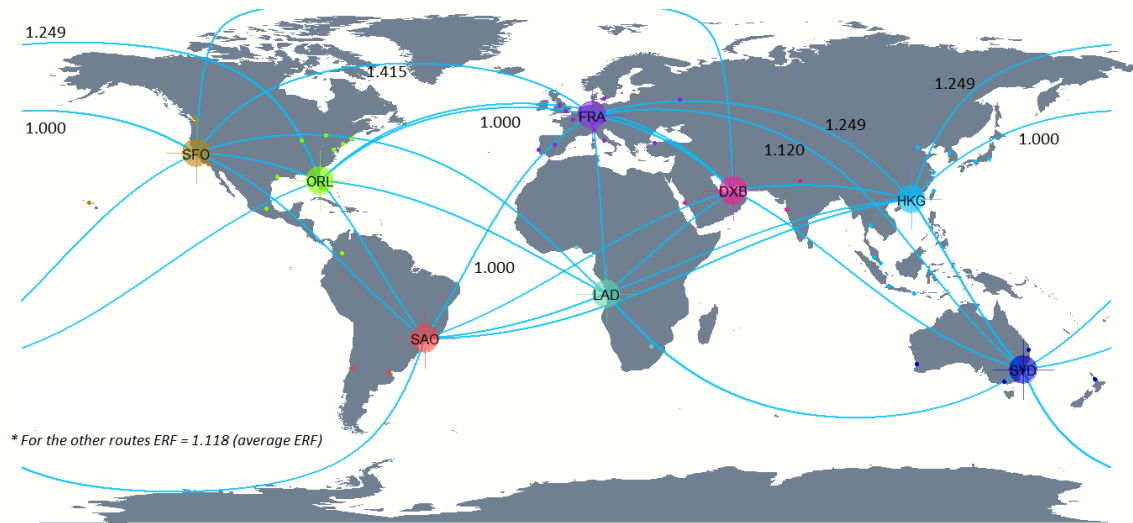
3.2.3 Robustness check: Sonic boom and flight path deviations

For robustness reasons, the distance computation is revised considering the particularities of the high-speed aircraft with respect to constraints imposed by sonic boom. More specifically, the model uses great circle distance to compute the distance between city-pairs. However, because of the sonic boom and the need to avoid flying over highly populated areas, the GC distance may not be adequate for many HIKARI legs.

First, all the HIKARI legs in the eligible network have been classified in 28 traffic flows. An example of a big traffic flow is North America, west side, to Europe. Second, representative city-pairs for each big traffic flow have been identified. Finally, extended range factors (ERFs)¹⁴ have been computed for 7 representative city-pairs, which are applied to all CPs belonging to each of these big traffic flows. For the remaining 21 traffic flows, a weighted average ERF is applied to all CPs belonging to these traffic flows.

Figure 16 displays the 28 traffic flows, used to group the ~4800 OD city-pairs, together with the city centres in each traffic region and the 7 ERFs used to recalculate the distance. For the remaining 21 traffic flows, the weighted average ERF is 1.118.

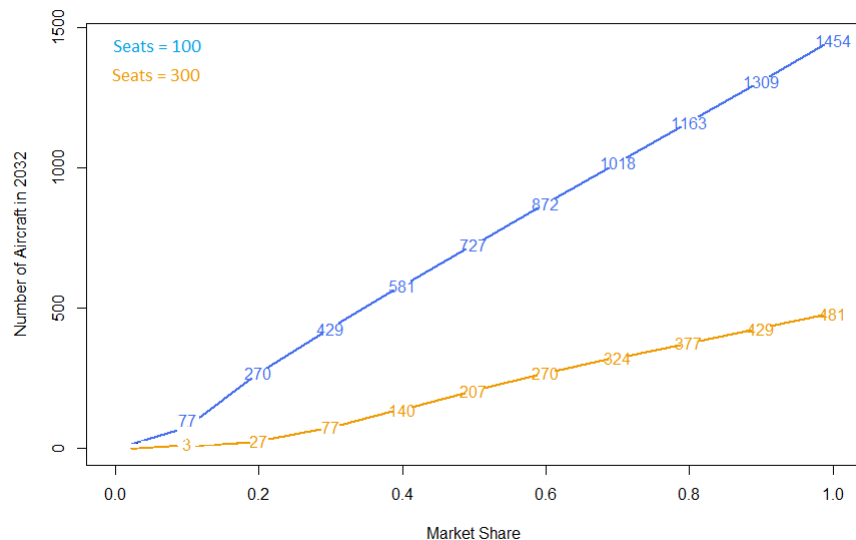
¹⁴ An extended range factor (ERF) is defined as the ratio between actual distance including flight path deviation and the GC distance.



Source: Airbus and ESA-ESTEC.

Figure 16: Traffic flows, city centres in each traffic region and ERFs

With the new flight distance computation, the forecasted number of aircraft is recalculated. The baseline scenario continues to be characterized by the following parameters: an average speed of 4200 km/h, an aircraft capacity of 100 seats, 3 weekly frequencies, 3150 yearly utilization hours and a load factor of 75%. We extend this baseline scenario, by allowing for an aircraft capacity of 300 seats. Figure 20 displays the results for cluster 1.

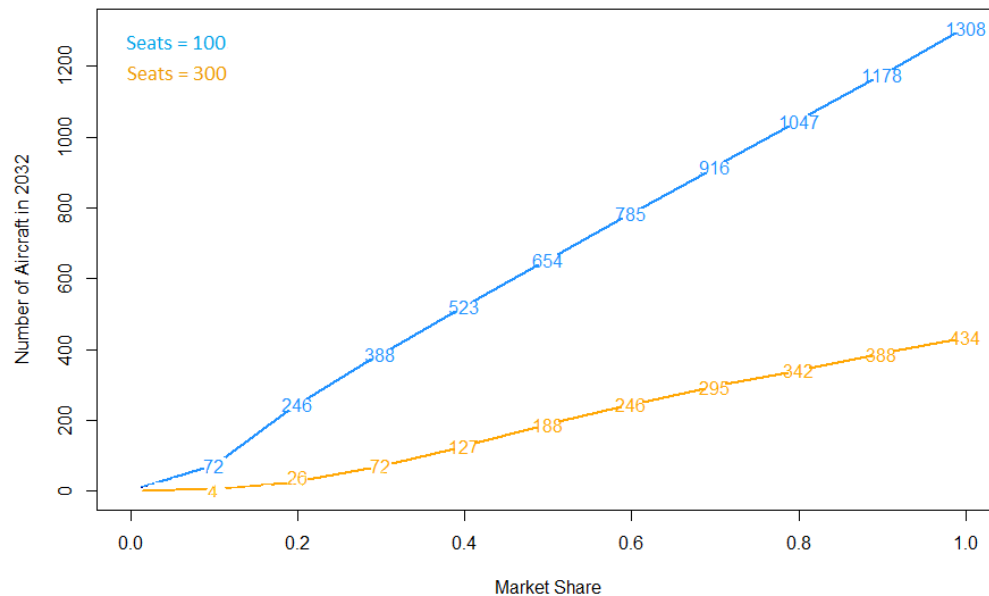


Assumptions: 3 weekly frequencies; aircraft capacity of 100 and 300 seats; load factor of 75%; Cluster 1, with an average speed of 4260 km/h.

Figure 17: Forecasted number of aircraft, in 2032, accounting for flight path deviations. Cluster 1.

As it becomes clear from the comparison between the previous figure, **Figure 12** and **Figure 13**, the alternative way to compute the distance does not significantly alter the forecasted number of aircraft. As an illustration, assuming a 20% market share and 100 seats, the new distance computation results in 270 forecasted aircraft in 2032, whereas the baseline scenario yielded 276 expected high-speed vehicles.

Intuitively, the reduction in the forecasted number of aircraft is due to the assumption that the distance of the connecting leg and the HIKARI leg has to be at most 40% larger than the direct OD distance. More specifically, when taking into account the flight path deviation, due to the sonic boom, ~3,000 routings over 18,810 are discarded, because they no longer satisfy this assumption. This in turn yields to a reduced number of forecasted high-speed vehicles. **Figure 18** displays the results for cluster 2.



Assumptions: 3 weekly frequencies; aircraft capacity of 100 and 300 seats; load factor of 75%; Cluster 2, with an average speed of 7100 km/h.

Figure 18: Forecasted number of aircraft, in 2032, accounting for flight path deviations. Cluster 2.

To conclude, the procedure presented here enables to have a better assessment of the true distance that a high-speed aircraft would need to fly to overcome regulatory restrictions. Nevertheless, in terms of forecasted number of aircraft, the impact is negligible, regardless of the vehicle speed considered.

3.3 Cost and Ticket Price Estimation Results¹⁵

Figure 19 and **Figure 20** display estimates of the cost of a one-way ticket on the LAPCAT concept based on 2012 prices. The assumptions underlying these estimates (other than the number of seats per plane) are the same as discussed above.

¹⁵ This section is based on Oxford Economics' cost and ticket price estimation results. The authors would like to thank Tom Rogers and Philip Thomas for sharing these results with us.

Ticket price versus vehicles built, 100 seats/plane

€ per one way long-haul trip

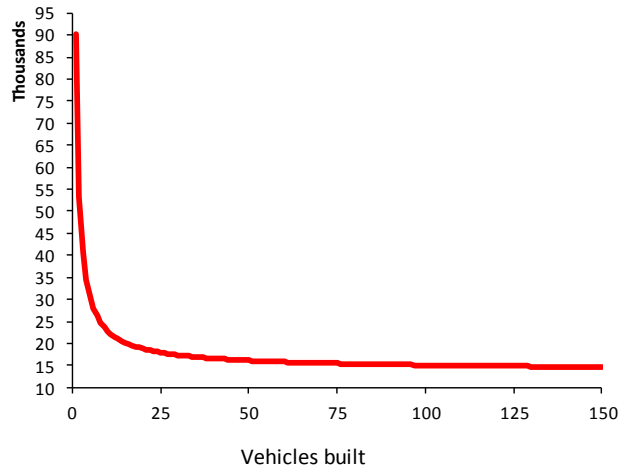


Figure 19: Ticket price versus vehicles built, 100 seats (Source: Oxford Economics.)

Ticket price versus vehicles built, 300 seats/plane

€ per one way long-haul trip

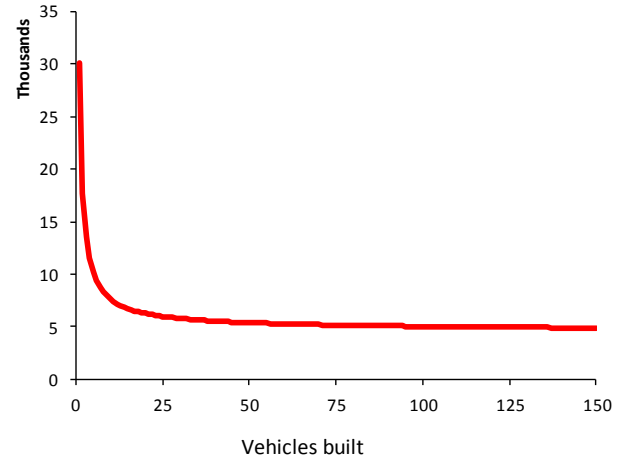


Figure 20: Ticket price versus vehicles built, 300 seats (Source: Oxford Economics.)

As demonstrated in the charts, there is a sharp fall in cost per ticket when moving from 0 to 15-20 or so vehicles. This is driven by two factors - the development costs being spread between ever more units and the “learning factor” pushing down unit costs as the production run is doubled from 1 to 2 units, 2 to 4, etc. However, both of these drivers become proportionately less important after around 20 units or so, as the impact of an extra unit on per vehicle development costs diminishes, and the intervals between doubling production runs widen dramatically. At this point the ticket price hits a floor, determined by variable costs such as the fuel bill per plane, and maintenance and other overheads. Specifically, in the case of a 300-seater vehicle this floor is around €5,000 per one-way trip, and in the case of a 100-seater vehicle, three times as much.

3.4 Market Share Capture Model

As already mentioned, the coefficients β_0 , β_1 and β_2 , as defined in section 2.4, were calibrated using Concorde data between 1984 and 2002. The value of the calibrated coefficients follow:

Coefficient	Value
β_0	0.000
β_1	0.939
β_2	0.692

Table 2: Calibrated coefficients of market share capture model (Source: Airbus)

Figure 21 and **Figure 22** display the estimated theoretical probability that an individual chooses a high-speed aircraft. As explained above, this probability depends on the flight time gain, relative to the subsonic aircraft, and the extra airfare that the passenger would need to pay to benefit from the flight

time reduction. Because this probability function is calibrated using Concorde data, **Figure 21** and **Figure 22** only provide a local approximation to the true probability. For a fare-ratio of 1 and a zero time-ratio, our market share capture model yields a probability of only 32%, far below the 100% that could have expected for this case. This lower percentage is probably due to the fact that only 2 airlines at the time, i.e. Air France and British Airways, offered a Concorde service, thus reducing the potential market capture. Hence the market share capture model should be considered as conservative.

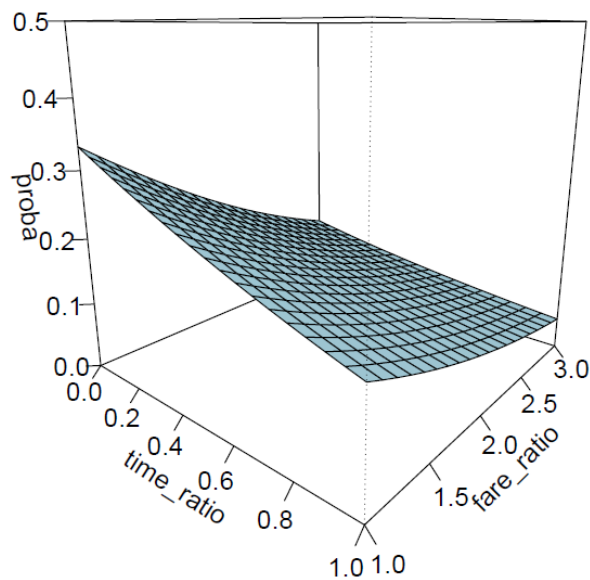


Figure 21: Market share capture model (Source: Airbus)

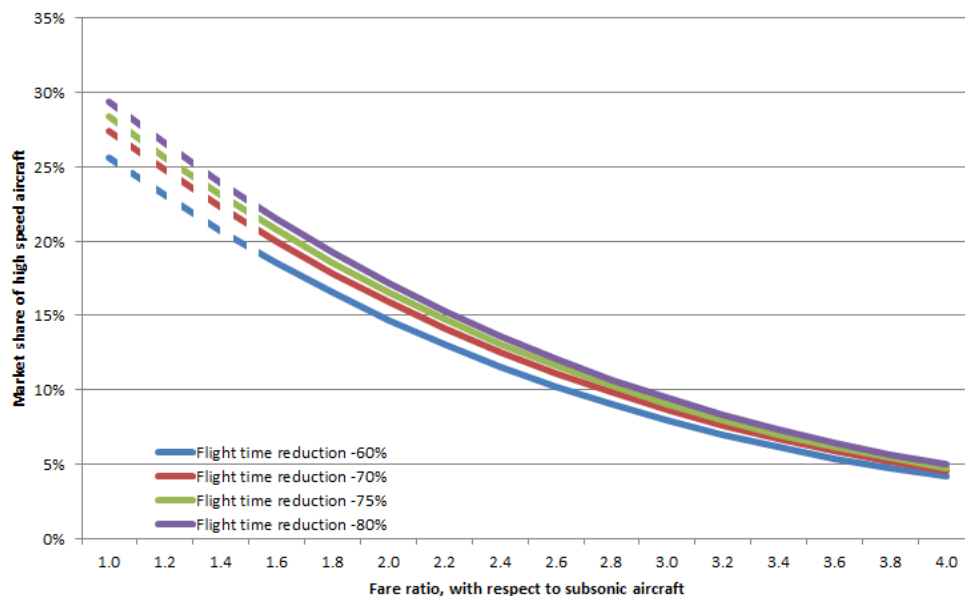


Figure 22: Estimated probability of market share capture (Source: Airbus)

The previous figures show that if the high speed aircraft is able to reduce the flight time by 75%, relative to a subsonic aircraft, while the ticket price increases by 400% (fare ratio of 4), the likely market share that the high speed vehicle would capture is ~5%.

Given the assumed average speed of 4260 km/h of cluster 1, the 75% time reduction is consistent with this cluster.¹⁶ Also, a fare ratio of ~4 is aligned with OE's ticket price estimation, assuming an aircraft capacity of 100 seats and provided an average FC+B ticket price of € 4,300 is supposed.¹⁷ The situation is slightly different if, instead, an aircraft capacity of 300 seats is considered. This is because a bigger aircraft implies a lower ticket price. The result is that, for a constant 75% time reduction, the likely market share of the high-speed vehicle would increase to ~13%, provided a fare ratio of 2.3¹⁸ is considered, or it would reach the ~26%, if the fare ratio equals 1.2.

Regarding cluster 2, with an average speed of 7100 km/h, the expected market share would be ~5% if the vehicle capacity has 100 seats; ~14% if 300 seats and a fare ratio of 2.3 are supposed and finally, ~27%, provided 300 seats and a fare ratio of 1.2 are considered. **Table 3** summarizes the previous results.

Table 3: Summary of market share capture model results Source: Airbus.

Average speed	Aircraft capacity	Fare ratio	Time reduction	Likely market share
Cluster 1	100 seats	3.9	-75%	~5%
	300 seats	2.3	-75%	~13%
	300 seats	1.2	-75%	~26%
Cluster 2	100 seats	3.9	-80%	~5%
	300 seats	2.3	-80%	~14%
	300 seats	1.2	-80%	~27%

3.5 Theoretical Equilibrium Determination: Expected Future Number of Aircraft based on Market Share and Ticket Price Models

By combining the results obtained in sections 3.1 to 3.4, section 3.5 offers a theoretical exercise to evaluate the market equilibrium, which is defined as a vector

$$E^* = (Ticket\ price^*, Market\ share^*, Number\ of\ aircraft^*).$$

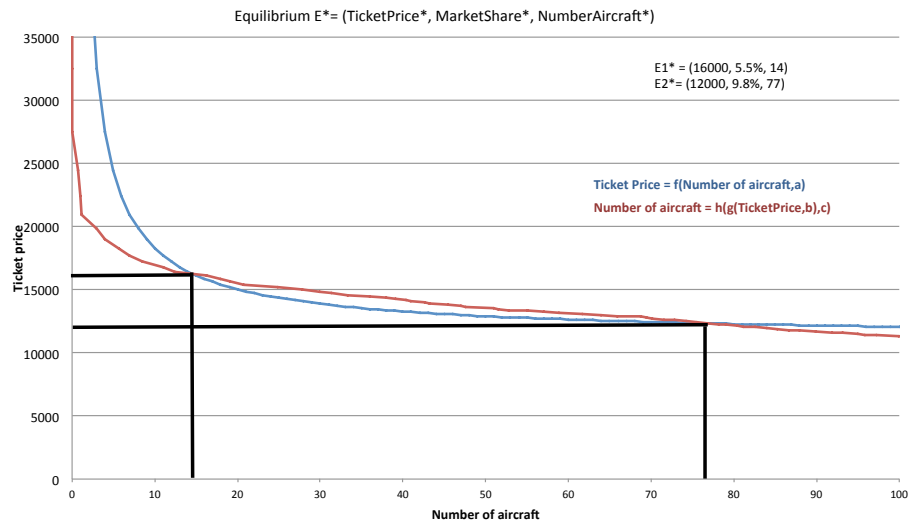
By plugging equation (2) into (3), **Figure 23** and **Figure 24** display the previous relationship, together with equation (1) and the equilibrium vectors for the case of 100 and 300 seats, respectively, and cluster 1. Importantly, figure 28 assumes that the development and production costs for a 100-seater aircraft

¹⁶ This is also in line with the fact that for cluster 1, the weighted average flight time ratio over the eligible OD CPs is 0.25.

¹⁷ More precisely, a ticket price for the high speed aircraft of €17,000 and an average FC+B ticket price of € 4,300 (both as of 2012 prices) result in a fare ratio of 3.9.

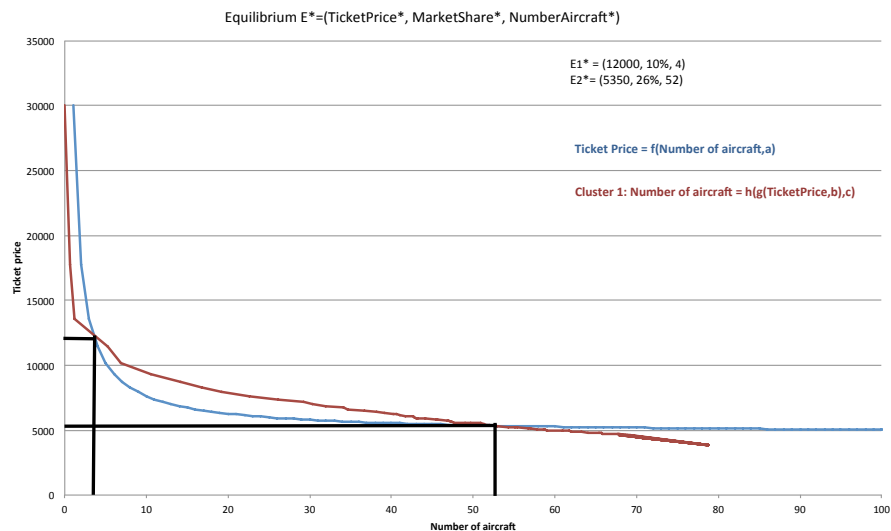
¹⁸ An average ticket price for the high speed aircraft of €10000, together with an average FC+B ticket price of € 4,300, yield a fare ratio of 2.3.

are 20% lower than for the 300-seater.¹⁹ Otherwise, there would be no equilibrium for the case of 100 seats.



Assumptions: 3 weekly frequencies; aircraft capacity of 100; load factor of 75%; Cluster 1, with an average speed of 4260 km/h.

Figure 23: Theoretical equilibrium determination, 100 seats, cluster 1.



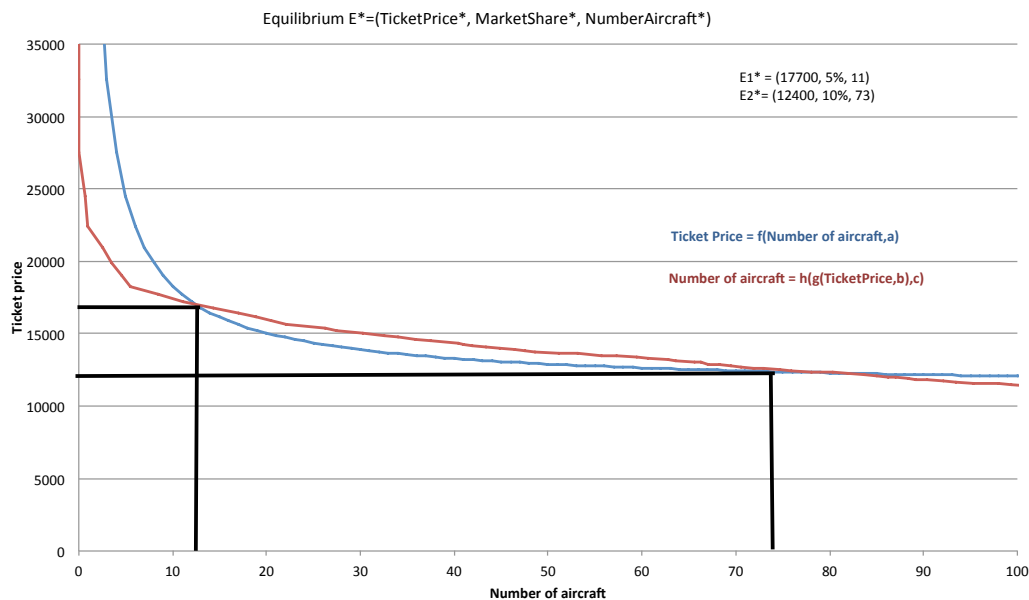
Assumptions: 3 weekly frequencies; aircraft capacity of 300 seats; load factor of 75%; Cluster 1, with an average speed of 4260 km/h.

Figure 24: Theoretical equilibrium determination, 300 seats, cluster 1.

¹⁹ 20% is the minimum development and production cost reduction that is required for at least one equilibrium to exist.

Figure 23 and **Figure 24** show that regardless of the aircraft capacity considered, there are two equilibria, that is, a low and a high equilibrium. The low equilibrium is characterized by a high-ticket price, low market share and few forecasted aircraft, whereas the high equilibrium yields a lower ticket price, a higher market share and more forecasted aircraft, relative to the low equilibrium.²⁰ What is crucial for this exercise is the ticket price determination, which in turn depends on the development and production costs, at which an aircraft manufacturer would be able to produce such a high-speed aircraft

Figure 25 and **Figure 26** depict the theoretical equilibrium vectors for cluster 2, assuming 100 and 300 seats, respectively. As before, figure 31 assumes that the development and production costs for a 100-seater aircraft are 20% lower than for the 300-seater.²¹

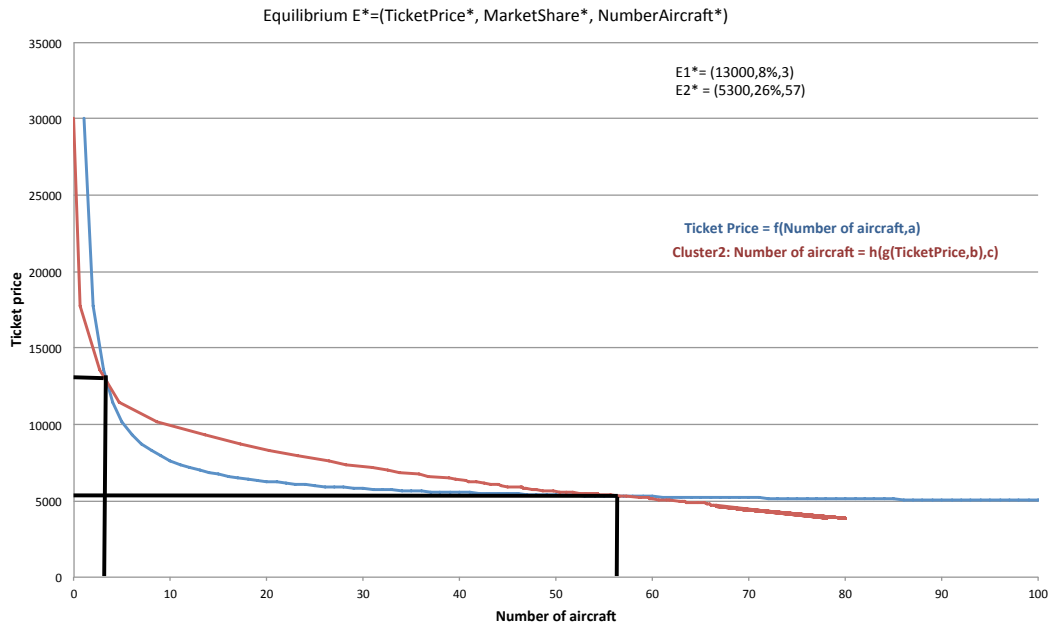


Assumptions: 3 weekly frequencies; aircraft capacity of 100 seats; load factor of 75%; Cluster 2, with an average speed of 7100 km/h.

Figure 25: Theoretical equilibrium determination, 100 seats, cluster 2.

²⁰ For comparison, the theoretical equilibrium determination for the scenario 300 seats, cluster 1 and 20% reduction in the development and production costs is depicted in the appendix.

²¹ The theoretical equilibrium determination of the scenario 300 seats, cluster 2 and 20% reduction in the development and production costs is also depicted in the appendix.



Assumptions: 3 weekly frequencies; aircraft capacity of 300 seats; load factor of 75%; Cluster 2, with an average speed of 7100 km/h.

Figure 26: Theoretical equilibrium determination, 300 seats, cluster 2

4 CONCLUSIONS AND WAY FORWARD

The market study shows that there is a market for a potential future high-speed transport aircraft. The following paragraphs and **Table 4** summarize the main results obtained in this paper:

1. Ticket prices decrease with aircraft capacity; with these obtained prices, the HST is economically competitive with the classically used aircraft with respect to premium passengers for 300-seater aircraft. For 100-seaters, an equilibrium is found at a 2.3 higher ticket price.
2. The results of the theoretical equilibrium determination show a trade-off between market share and aircraft units. More specifically, while the equilibrium market share is at most 10% for the 100-seater and 26% for the 300-seater aircraft, the number of deployed aircraft with the former (100-seater) is 77 compared to 54 for the latter (300-seater aircraft).
3. There is a negligible preference for a higher speed (cluster 2) on the market share over the lower speed (cluster 1)
4. Relying on Concorde dataset, the market share is at best limited to 32%. As the 300-seater passenger aircraft have equilibrium points (up to 26%) close to this maximum, the share would actually be larger if the limitation of 32% would be lifted.

Table 4: Summary of market study results

Concept		Result
Hikari Network	Total Traffic in 2032	4,105 OD CPs with 4,903,294 monthly passengers
	Local Traffic in 2032	268 OD CPs with 2,406,258 monthly passengers.
	Top 20 routes	696,855 passengers
	Average extended range factor	1.127
Average Flight Time Ratio per OD (HST/Subsonic)		Cluster 1: 0.255 Cluster 2: 0.190
Theoretical equilibrium determination $E^* =$ (Ticket Price*, Market Share*, Number of Aircraft*) \propto	Cluster 1, 100 seats	Equilibrium 1: (Ticket Price = 16000, Market Share = 5.5%, Number of Aircraft = 14) Equilibrium 2: (12000, 9.8%, 77)
	Cluster 1, 300 seats	Equilibrium 1: (12000, 10%, 4) Equilibrium 2: (5300, 25%, 52)
	Cluster 2, 100 seats	Equilibrium 1: (Ticket Price = 17700, Market Share = 5%, Number of Aircraft = 11) Equilibrium 2: (12400, 10%, 73)
	Cluster 2, 300 seats	Equilibrium 1: (13000, 8%, 3) Equilibrium 2: (5300, 26%, 54)

\propto : To determine the equilibrium, the following system of 3 equations, with 3 unknowns (Ticket price*, Market share*, Number of aircraft*) is solved:

- (1) Ticket price = f (Number of aircraft, a)
- (2) Market share = g (Ticket price, b)
- (3) Number of aircraft* = h (Market share, c); with a, b and c fixed parameters.

From this first market evaluation, three venues of future research are proposed.

The first one and most immediate is to extrapolate our results to consider a 2050 time frame. The reason for such an extension is that technology readiness at that point (~2050) should allow the high-speed aircraft to be ready for operational use. At least a preliminary assessment of the potential future market for a high-speed aircraft is therefore strongly desirable.

A second venue of future research is to conduct a dedicated survey to premium and tourist passengers rather than using a market share capture model calibrated on Concorde data. Such a technique could improve the value of time estimation, being more suitable for the HST context.

Finally, the performance and capabilities of the high-speed transportation was performed on overall values of the conceptual designs provided by the consortium. Making a dedicated assessment with the actual capabilities for each of the conceptual HST aircraft will indicate which of the designs and deployed technologies should be followed to assure the best value for the market.

Acknowledgments

The research leading to the results has received funding from the European Union Seventh Framework Programme (FP7/2007-2013) under grant agreement n° 313987 HIKARI, with the coordinated support from METI, the Ministry of Economy, Trade and Industry of Japan.

5 REFERENCES

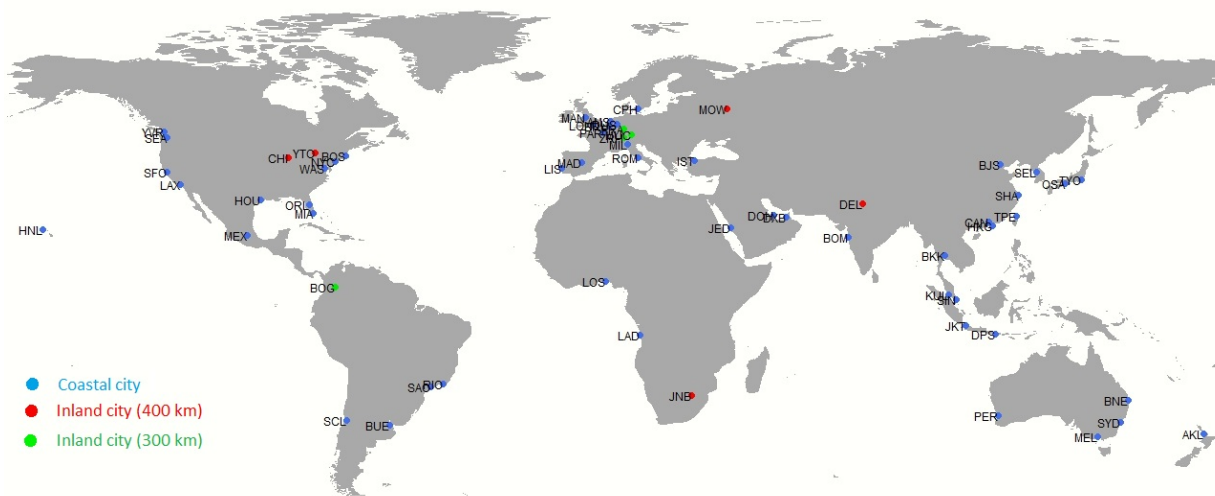
- [1] Steelant, J.: 'LAPCAT: High-Speed Propulsion Technology', RTO / AVT / VKI Lecture Series on Advances on Propulsion Technology for High-Speed Aircraft, Von Karman Institute, St. Genesius-Rode, Belgium, 12-15/03/2007.
- [2] Candel, S.: 'Concorde and the Future of Supersonic Transport', Journal of Propulsion and Power Vol. 20, No. 1, January–February 2004.
- [3] <http://www.concordesst.com/concordeb.html>
- [4] Steelant J.: 'ATLLAS: Aero-Thermal Loaded Material Investigations for High-Speed Vehicles', 15th AIAA International Space Planes and Hypersonic Systems and Technologies Conference, 28/04-01/05-2008, Dayton, Ohio, USA, AIAA-2008-2582.
- [5] Steelant J.: 'Achievements Obtained for Sustained Hypersonic Flight within the LAPCAT project.', 15th AIAA International Space Planes and Hypersonic Systems and Technologies Conference, 28/04-01/05-2008, Dayton, Ohio, USA, AIAA-2008-2578.
- [6] Steelant, J.: 'Sustained Hypersonic Flight in Europe: Technology Drivers for LAPCAT II', 16th AIAA/DLR/DGLR International Space Planes and Hypersonic Systems and Technologies Conference, October 19-22, 2009, Bremen, Germany, AIAA-2009-7206.
- [7] Mack A. and Steelant J.: 'FAST20XX: First Progress on European Future High-Altitude High-Speed Transport', 17th AIAA International Space Planes and Hypersonic Systems and Technologies Conference, April 11-14, 2011, San Francisco, USA, AIAA-2011-2337.
- [8] Defoort, S., L. Serre, R. Grenon, J. Varnier, G. Carrier, D. Scherrer, Narmada: 'ZEHST: Environmental Challenges for Hypersonic Passenger Transport'. 18th AIAA/3AF International Space Planes and Hypersonic Systems and Technologies Conference, 24 - 28 September 2012, Tours, France, AIAA-5873.
- [9] De Saint Marin, P., B. Stoufflet, Y. Dermaux, J. Négrier: 'Design of a Small Supersonic transport Aircraft with High Environmental Constraints', ICAS 2008.
- [10] Taguchi, H., Kobayashi, H., Kojima, T., Ueno, A., Imamura, S., Hongoh, M., Harada, K.: 'Systems Analysis on Hypersonic Airplanes using Pre-Cooled Turbojet Engine', 17th AIAA International Space Planes and Hypersonic Systems and Technologies Conference, April 11-14, 2011, San Francisco, USA, AIAA-2011-2320.
- [11] Airbus, Global Market Forecast 2013, 'Future Journeys', 2013.
- [12] Train, K.: 'Discrete choice models with simulations', Cambridge University Press, 2009.
- [13] Steelant, J.: 'Long-Term Advanced Propulsion Concepts and Technologies', AST4-CT-2005-012282 – Noordwijk, Netherlands – 2008.
- [14] Grosche, T.: 'Computational Intelligence in Integrated Airline Scheduling', Studies in Computational Intelligence, Volume 173, 2009.

- [15] Mathaisel, D. F. X.: Decision support for airline schedule planning. Journal of Combinatorial Optimization, 1, 251–275, 1997.
- [16] Schmitz, G., Kauthen, J.-P., Akkaya, N., Halsall, L.: NAPPA mini model guide. User Information. Zurich. 1998.

6 NOMENCLATURE

CP:	City-pair
ERF:	Extended range factor
ESA:	European Space Agency
FC+B:	First and business class
GC:	Great circle
GDD:	Global Demand Data
GMF:	Airbus Global Market Forecast
GVA:	Gross Value Added
HST:	High Speed Transport
OD:	Origin and Destination
OE:	Oxford Economics
RPK:	Revenue passenger kilometre
Sfc:	Specific Fuel Consumption

7 APPENDIX



Note: The name of the city, abbreviation and distance to the coast for each city follow: AKL-Auckland (7km), AMS-Amsterdam (21km), BJS-Beijing (145km), BKK-Bangkok (64km), BNE-Brisbane (24km), BOG-Bogota (333km), BOM-Mumbai (18km), BOS-Boston (6km), BRU-Brussels (53km), BUE-Buenos Aires (17km), CAN-Guangzhou (42km), CHI-Chicago (964km), CPH-Copenhagen (4km), DEL-Delhi (816km), DOH-Doha (55km), DPS-Denpasar Bali (6km), DUS-Duesseldorf (142km), DXB-Dubai (102km), FRA-Frankfurt (332km), HKG-Hong Kong (2km), HNL-Honolulu (13km), HOU-Houston (22km), IST-Istanbul (22km), JED-Jeddah (63km), JKT-Jakarta (90km), JNB-Johannesburg (436km), KUL-Kuala Lumpur (47km), LAD-Luanda (23km), LAX-Los Angeles (18km), LIS-Lisbon (16km), LON-London (52km), LOS-Lagos (15km), MAD-Madrid (299km), MAN-Manchester (29km), MEL-Melbourne (24km), MEX-Mexico City (241km), MIA-Miami (20km), MIL-Milan (121km), MOW-Moscow (645km), MUC-Munich (305km), NYC-New York

(20km), ORL-Orlando (55km), OSA-Osaka (12km), PAR-Paris (153km), PER-Perth (34km), RIO-Rio De Janeiro (15km), ROM-Rome (83km), SAO-Sao Paulo (81km), SCL-Santiago (87km), SEA-Seattle (4km), SEL-Seoul (25km), SFO-San Francisco (19km), SHA-Shanghai (41km), SIN-Singapore (3km), SYD-Sydney (73km), TPE-Taipei (22km), TYO-Tokyo (12km), WAS-Washington (10km), YTO-Toronto (536km), YVR-Vancouver (11km), ZRH-Zurich (337km)

Figure 27 : Eligible HIKARI cities, with distance to the coast.

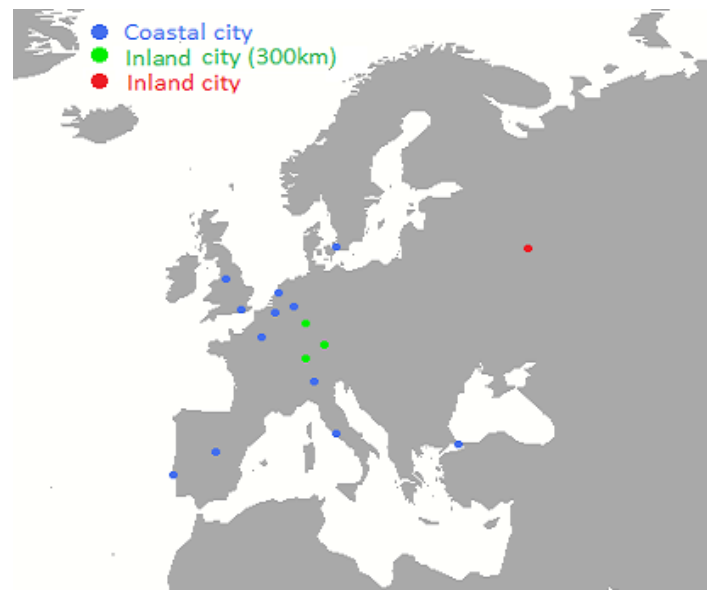
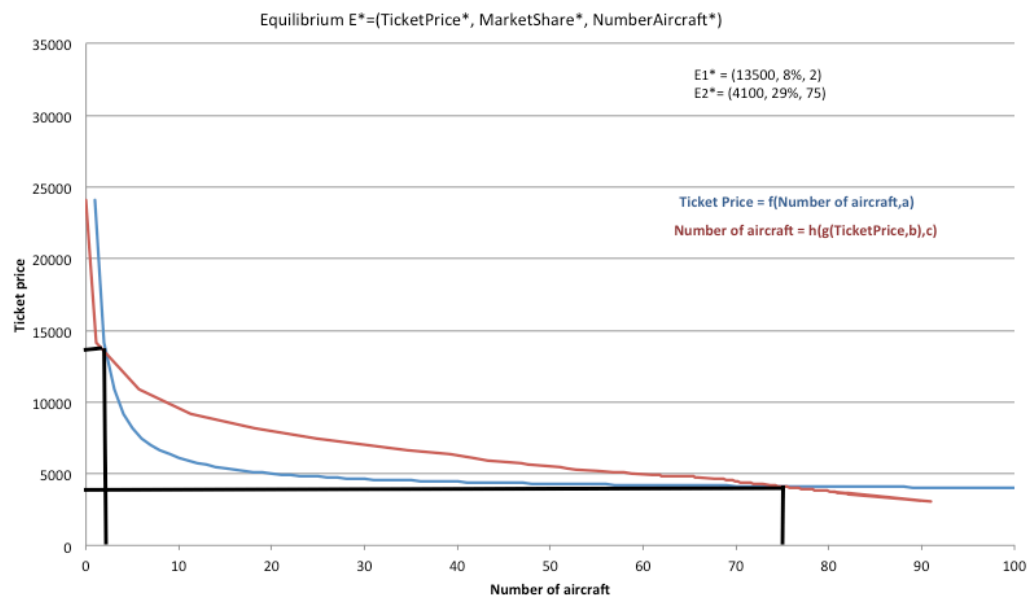
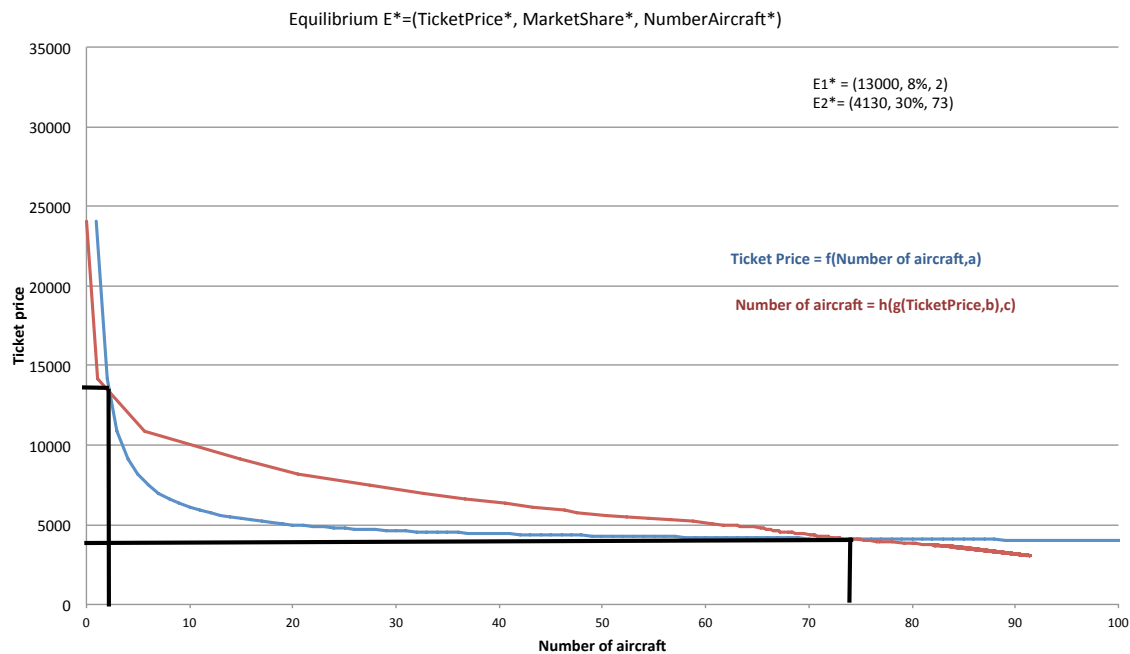


Figure 28 : Eligible HIKARI cities, Europe in detail.



Assumptions: 3 weekly frequencies; aircraft capacity of 300 seats; load factor of 75%; Cluster 1, with an average speed of 4260 and 20% reduction in the development and production costs.

Figure 29 : Theoretical equilibrium determination, 300 seats, cluster 1



Assumptions: 3 weekly frequencies; aircraft capacity of 300 seats; load factor of 75%; Cluster 2, with an average speed of 7100 and 20% reduction in the development and production costs.

Figure 30 : Theoretical equilibrium determination, 300 seats, cluster 2